Bioactive Materials 6 (2021) 3801–3811

Contents lists available at ScienceDirect

Bioactive Materials

journal homepage: www.sciencedirect.com/journal/bioactive-materials

Hyaluronic acid facilitates bone repair effects of calcium phosphate cement by accelerating osteogenic expression

Xu Cui [a,1], Chengcheng Huang [a,1], Zhizhen Chen [a,1], Meng Zhang [a], Chunyu Liu [a], Kun Su [a], Jianyun Wang [b], Li Li [c], Renxian Wang [d], Bing Li [c], Dafu Chen [d], Changshun Ruan [a], Deping Wang [e], William W. Lu [a,f], Haobo Pan [a,*]

[a] Center for Human Tissues and Organs Degeneration, Shenzhen Institutes of Advanced Technology, Chinese Academy of Science, Shenzhen, 518055, PR China
[b] Shenzhen Healthemes Biotechnology Co. Ltd, Shenzhen, 518102, PR China
[c] Department of Orthopedics, Fourth Affiliated Hospital of Guangxi Medical University/Liu Zhou Worker, Liuzhou, 545005, PR China
[d] Laboratory of Bone Tissue Engineering Beijing, Laboratory of Biomedical Materials, Beijing Research Institute of Orthopaedics and Traumatology, Beijing Jishuitan Hospital, Beijing, 100035, PR China
[e] Schools of Materials Science and Engineering, Tongji University, Shanghai, 201804, PR China
[f] Department of Orthopaedics and Traumatology, The University of Hong Kong, Hong Kong SAR, PR China

ARTICLE INFO

Keywords:
Hyaluronic acid
Calcium phosphate cement
Physicochemical properties
Osteogenic activity

ABSTRACT

Calcium phosphate cements (CPC) are widely anticipated to be an optimum bone repair substitute due to its satisfied biocompatibility and degradability, suitable to be used in minimally invasive treatment of bone defects. However the clinical application of CPC is still not satisfied by its poor cohesiveness and mechanical properties, in particular its osteoinductivity. Hyaluronic acid reinforced calcium phosphate cements (HA/CPC) showed extroadinary potential not only enhancing the compressive strength of the cements but also significantly increasing its osteoinductivity. In our study, the compressive strength of HA/CPC increased significantly when the cement was added 1% hyaluronic acid (denoted as 1-HA/CPC). In the meantime, hyaluronic acid obviously promoted ALP activity, osteogenic related protein and mRNA expression of hBMSCs (human bone marrow mesenchymal stem cells) *in vitro*, cement group of HA/CPC with 4% hyaluronic acid adding (denoted as 4-HA/CPC) showed optimal enhancement in hBMSCs differentiation. After being implanted in rat tibial defects, 4-HA/CPC group exhibited better bone repair ability and bone growth promoting factors, comparing to pure CPC and 1-HA/CPC groups. The underlying biological mechanism of this stimulation for HA/CPC may be on account of higher osteogenic promoting factors secretion and osteogenic genes expression with hyaluronic acid incorporation. These results indicate that hyaluronic acid is a highly anticipated additive to improve physicochemical properties and osteoinductivity performance of CPCs for minimally invasive healing of bone defects.

1. Introduction

Large bone defects, the clinical challenges to enhance bone quality, mainly arisen by trauma, malignancy, infection and congenital diseases are frequently occurrences in orthopedic and craniofacial surgery [1]. Until now, autologous bone grafts and allografts are still highly priority in the treatment of large bone defects, even though they suffer from limitations including short supply, donor site morbidity, immunogenicity and possible disease transmission and immune reaction [2]. Therefore it's becaming dramatically exigent to develop biomaterials as bone graft that satisfy different bone repair needs.

Among various types of commercial injectable bone grafts, calcium phosphate cement (CPC) has been paid widely attention due to its similarity to nature bone since developed in 1980s by Chow [3]. After setting, it can spontaneously bonding with bone tissues by the formation of hydroxyapatite-like mineral [4,5], the thermodynamic stable phase in calcium phosphates. However, the brittleness and less osteogenesis of CPC restrict wider application due to its poor cohesiveness,

Peer review under responsibility of KeAi Communications Co., Ltd.
* Corresponding author.
E-mail address: hb.pan@siat.ac.cn (H. Pan).
[1] These authors are contributed equally to this work.

https://doi.org/10.1016/j.bioactmat.2021.03.028
Received 5 February 2021; Received in revised form 8 March 2021; Accepted 16 March 2021

non-sufficient mechanical properties and lack of osteoinductivity [6]. Many studies have attempted to improve physicochemical properties, such as mechanical properties and cohesiveness, and biological performance of CPC [4–8]. It was reported that polymers, especially the natural biopolymers, dissolved in the setting liquid of the starting mixture, could react during the setting process to form an interconnecting hydrogel matrix within the porous cement structure, which might lead to an increase in the compressive strength of the cement after setting [9]. Moreover, adding an organic phase such as carboxymethyl cellulose (CMC), gelatin, chitosan, or konjac glucomannan to CPC could also improve the washout resistance of the cement [10–12].

Incorporation of natural biopolymers such as hyaluronic acid (HA) into the cement matrix has also been found to be an attractive approach [13]. Hyaluronic acid is a natural linear glycosaminoglycan with high hydrophilicity, non-toxicity, non-immunogenicity and good biocompatibility [14]. Besides, hyaluronic acid is one of the major components of extracellular matrix (ECM) in mammalian connective tissues, fulfilling both physiochemical and biological functions [14]. Through direct or indirect interactions with specific binding proteins, such as CD44, transforming growth factor-β (TGF-β) and so on [15], hyaluronic acid can stimulate cell adhesion, proliferation and differentiation [16]. After being implanted *in vivo*, hyaluronic acid could modulate differentiation of bone marrow mesenchymal stem cells (BMSCs) to accelerate healing of cranial bone defects [17,18]. Moreover, the degradation products of hyaluronic acid have been reported to induce an angiogenic response (formation of new blood vessels) on the chick chorioallantoic membrane [19].

While these results are inspiring, the proper amount of hyaluronic acid (HA) in calcium phosphate cement to achieve the optimal physicochemical properties and ability to stimulate bone repair still needs to be discussed, and the underlying biological mechanism of this stimulation of hyaluronic acid incoporating into calcium phosphate cement is yet to be determined.

Therefore, this study was aimed to conduct the effects of hyaluronic acid on physicochemical properties and osteogenic capacity of a calcium phosphate cement. Firstly, cements composed of biphasic phosphate particles and citric acid liquid phase incorporated with varying amounts of hyaluronic acid (0–4 wt %) were selected. Subsequently, hydroxyapatite conversion, compressive strength and handling properties of the cements were evaluated *in vitro*. Then the ability of hyaluronic acid in the cements to affect proliferation, differentiation and mineralization of human bone marrow stem cells (hBMSCs) was studied *in vitro*. Cements were implanted for 4, 8 and 12 weeks in a rat tibial defect to evaluate the healing effects as follow.

2. Materials and methods

2.1. Fabrication of hyaluronic acid/calcium phosphate cements

The hyaluronic acid/calcium phosphate (HA/CPC) cements were composed of biphasic calcium phosphate powder (solid phase) and a liquid phase. The biphasic calcium phosphate powder contained tetracalcium phosphate (TTCP) (Sigma-Aldrich) and dicalcium phosphate anhydrous (DCPA) (Sigma-Aldrich) in a 1:1 ratio in molar acorrding to our previous research [6]. The biphasic calcium phosphate powder was produced through mixing TTCP and DCPA in a planetary ball milling (QM-3SP2, Nanjing NanDa) at 360 rpm for 2 h. The cement liquid phase was prepared by dissolving hyaluronic acid powder (97%, ~100 KDa, Shanghai Macklin Biochemical Industry Co., Ltd) in a citric acid solution. The citric acid solution (20%, w/v, pH = 4) was produced by dissolving acid monohydrate (Sinopharm) in deionized water with 0.1 M NaOH (Sinopharm) adjusting its pH value. After being stirred for 10–20 min, 0%, 1% and 4% (w/v) hyaluronic acid was added to the citric acid solution. The mixing solution was stored at 4 °C after continuous stirring for future use. Pasty adhesive was prepared by stirring the biphasic calcium phosphate powder and the liquid phase in a plastic bowl for about 2.0 min using a pestle. A fixed ration of solid phase to liquid phase (weight to volume ratio) was 2:1 g/ml for each cement group acorrding to our previous research [6]. Then the cement paste was filled into polytetrafluoroethylene molds of different sizes (such as the size of 12 mm × 3.0 mm) and allowed for setting for 30 min. The cement samples were taken out and dried for 24 h at room temperature for future use. The composition of hyaluronic acid/calcium phosphate cements are listed in Table 1.

2.2. Handling properties of hyaluronic acid/calcium phosphate cements in vitro

Injectability of the cement paste was measured *in vitro* using a method described previously [20]. Briefly, the prepared cement pastes, as described above, was placed into a 2.5 ml syringe (Kindly Enterprise Development Group Co., Ltd) with an opening diameter of 1.7 mm. To injected out of the paste, a force of 150 N was applied vertically at syringe piston with a crosshead speed of 5 mm/min using a universal tester (ZHIQU Test Machine Inc.). The injectability (Ij) of the cement paste was calculated using equation (1), where Wo is the initial weight of the paste in the syringe, and W is weight of remaining paste in the syringe after the injection. For injectability test, 6 samples were used as duplicate and the results are expressed as a mean ± SD.

$$Ij = \frac{Wo - W}{Wo} * 100\% \quad (1)$$

To test the initial setting time (IST) of cements, pastes prepared as presented above was extruded in a Teflon mold with size of 20 mm in diameter and 5 mm in height and placed in constant temperature (37 °C) and humidity (60%) chamber. IST was determined using Gilmore method according to ASTM C266-2007. For IST test, 6 samples were used as duplicate and the results are expressed as a mean ± SD.

2.3. Hydroxyapatite conversion and bioactivity of hyaluronic acid/calcium phosphate cements in vitro

Hydroxyapatite conversion and bioactivity of different cement groups was evaluated as a function of immersing time in phosphate buffer solution at 37 °C. Cement samples with size of 12 mm in diameter and 3 mm in height) were immersed in 33.9 ml PBS (The calculation is based on references [21]) in sterile polyethylene containers, with one sample per container. At selected time point, cement samples were taken out, washed with deionized water and dried at room temperature. 5 samples were used as duplicate and the results were showed as mean ± SD. Surface and cross-sections morphological features of the cements before and after being immersed in PBS were characterized by field emission scanning electron microscope (FE-SEM) (Nova NanoSEM 450, FEI). Hydration and conversion of hydroxyapatite in the cements before and after being immersed in PBS was measured by X-ray diffraction method (D/max-2500VB2+/PC, Rigaku). Monochromatic Cu Kα radiation (λ = 0.15406 nm) was used and the scanning rate was 8° min^{-1} (in the range of 10–80° 2θ).

2.4. Compressive strength of hyaluronic acid/calcium phosphate cements

Compressive strength of the as-prepared cements was tested in a

Table 1
Composition of hyaluronic acid/calcium phosphate cements.

Cements	Solid phase (g)	Setting liquid (ml)		
Composition	TTCP: DCPA = 1:1 (molar ratio)	hyaluronic acid (g)	Citric acid solution (ml)	pH
CPC	2	0	1	4
1-HA/CPC	2	0.01	1	4
4-HA/CPC	2	0.04	1	4

universal tester (ZHIQU Test Machine Inc) *Vs* immersing time umtil 21 days in PBS. Cylindrical samples (6 mm × 12 mm) were immersed in 28.3 ml PBS (The calculation is based on references [21]) in sterile polyethylene containers (one sample per container). Five samples per group were subjected to testing at a crosshead speed of 1.0 mm/min at each time point. Compressive strength per sample was finally expressed as mean ± SD.

2.5. In vitro response of human bone marrow mesenchymal stromal cells (hBMSCs) to hyaluronic acid/calcium phosphate cements

2.5.1. Cell culture

The hBMSCs(ATCC®, PCS-500-012™) were cultured in α-MEM medium (Corning) with 10% fetal bovine serum (FBS; GIBCO, Australia) and 1% Penicillin-Streptomycin Solution (GIBCO). The cell digestion by using Trypsin EDTA solution (HyClone). The 6–8 generation of hBMSCs were cultured at normal cell incubator environment (37 °C, 5% CO_2 and 95% air). For the osteogenic induction studies, hBMSCs were cultured in the α-MEM medium for 3 days. After that, the cell medium was displaced by osteogenic inducing medium (OIM). OIM was prepared by adding 10% FBS and 1% Penicillin-Streptomycin Solution, 10 mM β-glycerolphosphate (Sigma-Aldrich), 50 μM ascorbic acid (Sigma-Aldrich), and 100 nM dexamethasone (Sigma-Aldrich) into α-MEM. All of the cement specimens used in this study were sterilized by 75% alcohol.

2.5.2. Cell adhesion and proliferation

The hBMSCs were cultured and seeded on tablet samples (10 mm × 3 mm) of each cement group with 5×10^4 cells per well in 24-well tissue culture plates. The hBMSCs were incubated in α-MEM medium with 10% FBS. The cells were cultured at normal cell incubator environment (37 °C, 5% CO_2 and 95% air). After 1 h and 24 h, specimens with cells were washed two times with PBS, and treated with 10% neutral formalin (BOSTER) for 15 min at room temperature, then washed three times with PBS. After being dehydrated in different grade of ethanol (50%, 70%, 90%, 95%, 100% ethanol in water, dehydrated for 5 min twice with each grade), and dried in a freeze dryer, the samples were coated with gold and tested in a FE-SEM (Nova NanoSEM 450, FEI). The hBMSCs proliferation was evaluated by CCK-8 assay (TransGen Biotech). Briefly, CPC, 1-HA/CPC, 4-HA/CPC samples (10 mm in diameter × 3 mm in height) were immersed in α-MEM with 10% FBS (0.2 g/ml) at 37 °C in the cell incubator for 24 h to obtain the cement extracts with extration ration (surface area of samples/volume) of 1.25 cm^2/ml according to ISO 10993. hBMSCs with density of 5×10^3 cell/well were seeded and incubated in α-MEM medium with 10% FBS in 96-well plates. After 24 h, the cell medium was displaced with the cement extracts. With another culture time of 1, 3 and 5 days respectively, the extracts in plates were replaced with fresh cell medium containing 10% CCK-8. After incubation for another 2 h in the cell incubator, the absorbance was measured at 450 nm by Multiskan Spectrum Microplate Spectrophotometer (Thermo Scientific). The cell medium without extract was used as the control.

2.5.3. Osteogenic differentiation

The hBMSCs were co-cultured with sterilized cement samples (12 mm × 3 mm) in 6-well plates with 1×10^5 cells per well in α-MEM medium with 10% FBS. The cell cultures were maintained att cell incubator environment (37 °C, 5% CO_2 and 95% air). After the cell confluence researched approximately 80%, the culture medium was change into OIM to induce differentiation of hBMSCs. After being incubated in OIM for 7, 14 and 21 days, OIM was discarded and the cells were washed two times with PBS. Differentiation of hBMSCs was tested with ALP activity and ALP stain.

ALP activity was examined with ALP detection kit (Beyotime Biotechnology). After 7 days of incubation, cells were lysed, and the ALP assay referred to the kit protocol (Beyotime Biotechnology). The total cellular protein was quantified simultaneously by BCA protein assay kit (thermo fisher scientific). The ALP activity results were normalized by total cellular protein. The culture medium without cement sample was used as the control. ALP staining was performed according to ALP staining kit protocol (Beyotime Biotechnology). After 7 days of incubation, the cell monolayer was washed two times with PBS and treated with 10% neutral formalin for 15 min at room temperature. After being washed two times with PBS, the cell samples were stained refer to ALP staining kit protocol and visualized with optical microscope (Axioskop 40; Carl Zeiss). The culture medium without cement sample was used as the control.

2.5.4. Expression of the osteogenic-related protein

Runt related transcription factor 2 (RUNX-2), Osteopontin (OPN) expression of hBMSCs was assessed by immunofluorescence assay (IF) after being co-cultured with cement samples for 7 days in OIM. After 7 days of incubation, the cell monolayer was washed two times with PBS, and treated with 10% neutral formalin for 15 min at room temperature. After being washed two times with PBS, the cell samples were incubated in blocking buffer (Beyotime Biotechnology) for 10 min. After that, cells were treated with anti-RUNX-2 and anti-OPN antibody solution (1: 100, Abcam) overnight at 4 °C, followed by incubation with secondary antibodies, goat anti-rat IgG with Alexa Fluor 488 (Abcam) for 1 h at room temperature, after that treated with rhodamine phalloidin (Invitrogen). The nucleus were stained by DAPI (Sigma-Aldrich). Expression of RUNX-2 and OPN was visualized using fluorescence Microscope (Olympus BX53, Olympus Global). The culture medium without cement samples was used as the control.

2.5.5. Expression of the osteogenesis-related genes

Osteogenic-related gene of hBMSCs treated with cements in OIM was detected by Quantitative reverse transcription-polymerase chain reaction (qRT-PCR). After being treated for 7, 14 and 21 days, the cell sample collection was used by AllPure Cell Kit (Magen) to extract the total RNA in cell samples. The RNA reverse-transcribed into complementary DNA (cDNA) was used by aRevert Aid First Strand cDNA Synthesis Kit (Thermo Fisher Scientific). qRT-PCR was performed to examine the gene expressed level of RUNX-2, OPN, ALP, and human β-actin was used as reference. Primer sequences information is listed in Table 2.

2.6. In vivo evaluation of hyaluronic acid/calcium phosphate cements

2.6.1. Animal model and implantation procedure

The animal experiment was obtained approval to execute in Shenzhen Institutes of Advanced Technology, Chinese Academy of Science. 27 adolescent female rats (3 months old, 250 ± 25 g) were used. The rats were kept separately in a stainless steel cage with metal wires at a temperature of 22 °C, with a 12 h/12 h light/dark cycle. All of rats were allowed to move, eat and drink freely after the operation. Upon arrival, the rats acclimated for seven days before initiation of the study. The sites for implantation were cleaned with 70% ethanol and betadine TM (10% povidone iodine). All of the animals underwent intraperitoneal surgery for general anesthesia with pentobarbital sodium (0.1 ml per 100 g, Tokyo Kasei Kogyo).

The cement specimens that already solidified (CPC, 1-HA/CPC, 4-

Table 2
The sequences of genes (F: forward primer R: reverse primer).

Gene	primer	Primer sequences (5'→3')
ALP	F	ACCACCACGAGAGTGAACCA
	R	CGTTGTCTGAGTACCAGTCCC
RUNX-2	F	TGGTTACTGTCATGGCGGGTA
	R	TCTCAGATCGTTGAACCTTGCTA
OPN	F	ACGCCGACCAAGGAAAACTC
	R	GTCCATAAACCACACTATCACCTCG
β-actin	F	CATGTACGTTGCTATCCAGGC
	R	CTCCTTAATGTCACGCACGAT

HA/CPC) were implanted in the metaphyseal region of medial tibia for both hind limbs. A longitudinal incision was made on the anterior surface of the tibia. The periosteum was then excised and a 2 mm guide hole was drilled with a thorn of 2 mm diameter. A ring was inserted at a depth of 2 mm to ensure the proper depth (2 mm) of the hole. After the cement sample (2 mm × 2 mm) was implanted, the subcutaneous tissue and skin were closed layer by layer with a silk thread. The rats were then subcutaneously injected with antibiotics (penicillium; Tai Yu Chemical & Pharmaceutical) at a dose of 40 mg/kg for 5 days, so as to reduce the risk of perioperative infection. Excessive amounts of barbiturates (Mebumal; ACO Läemedel AB) were given 4, 8, and 12 weeks after implantation. The implants in the metaphyseal region of medial tibia were taken out, and 9 rats were sacrificed at each time point for implantation.

2.6.2. Micro-computed tomography (micro-CT) analysis

The tibias of the rats were removed and placed in 10% formalin (BOSTER) for 24 h of fixing at room temperature. The reconstructed tibias were assessed by micro CT (SkyScan 1176, Bruker microCT) with a 18° m resolution for scanning. Feldkamp convolution back projection algorithm was used to reconstruct the image and adaptive local thresholding was used to segment into binay images. Ratio of new bone volume to tissue volume (BV/TV), bone mineral density (BMD) and bone trabecular pattern factor (Tb.pf) were calculated.

2.6.3. Histological analysis

The harvested tibia was treated in 10% formalin (BOSTER) at room temperature for 24 h. Afterwards the tibias were decalcified with neutral EDTA solution for about 4 weeks, and then dehydrated by different grade ethanol (70%, 80%, 90%, 95% and 100% ethanol in water). The dehydrated specimens were embedded in paraffin. Transverse sections of the specimens were cut, hand-grounded and polished to a final thickness of approximately 5 μm. Hematoxylin-eosin staining (H&E staining) and Masson's trichrome staining (MST Staining) were performed for histological analysis.

2.6.4. Immunohistochemical analysis

The prepared slides were rehydrated, and immumohistochemistry staining (IHC) was applied to examine the protein expressed level of Collagen I (COL-I), Osteocalcin (OCN) and Bone morphogenetic protein-2 (BMP-2). Briefly, the rehydrated slides were heated in sodium citrate buffer (Abcam) for antigen retrieval. Then the slides were washed with PBS, followed by being exposed to 5% BSA for 1 h at 37 °C to block non-specific binding. After that the slides were incubated with primary antibodies at 4 °C overnight, followed by incubation with 50 μL of mouse-anti rabbit-horseradish peroxidase (HRP) (BOSTER) for 50 min at room temperature. The reaction products were visualized with 3-3′ diaminobenzidine (DAB) (BOSTER) according to the manufacturer's instructions. The antibodies were diluted as follows: OCN antibody (1: 500, Abcam), BPM-2 antibody (1: 200, Beyotime) and COL-I antibody (1: 200, Beyotime). Quantification data of IHC were performed by calculating the mean optical density value of positive-staining areas. The area of interest was firstly focused on the new formed issue between the host bone and cement implant, then areas (n = 5) with remarkably high immunohistochemical staining were selected and manually quantified using the Image-Pro Plus software (Media Cybernetics).

2.7. Statistic analysis

All data were shown as means ± SD. Statistical significance was determined with one-way ANOVA and the Student's t-test. If $P < 0.05$, it was considered statistically significant.

3. Results

3.1. Handling properties

Dates for handling properties of cements with different hyaluronic acid (HA) incorporating were listed in Table 3. The average injectability of cement increased tremendous with hyaluronic acid (HA) incorporating, from 65.63 ± 3.51% for CPC group, to 83.68 ± 4.36% for 1-HA/CPC group. However, further incorporating of HA showed no significant increase in injectability, as injectability of 4-HA/CPC was 85.13 ± 3.89%. The initial setting time of cements decreased with HA incorporating, from 27.24 ± 0.98 min for CPC group, to 23.64 ± 0.76 min for 1-HA/CPC group. It seemed that more HA had a side effect on setting procedure, on the basis of prolonged initial setting time for 4-HA/CPC (24.56 ± 0.69 min).

3.2. Hydroxyapatite conversion and bioactivity

After immersion in PBS, TTCP and DCPA involved in CPC typically continued to hydrate and convert to hydroxyapatite, which was intermitted after setting of CPC [22]. Surface morphology of cement before and after immersion in PBS was depicted in Fig. 1a. The surface of the prepared cement was rough, with visible particles and micro/-macropores concentrated on the surface. After being immersed in PBS for 7 days, a layer of needle-like particles was deposited on the surface of the CPC sample, and a layer of flaky particles were observed on the surface of the 1-HA/CPC and 4-HA/CPC samples. Lengthening the immersing time in PBS generated the bigger size particles deposited on cement surface. Moreover, flaky particles on surface of 4-HA/CPC group emerged a bigger and more obvious morphology both at immersing time of 14 and 21 days. Cross-section morphology of the prepared cements (Fig. 1b) showed feature of inregular small crystals crisscrossing and connecting mutually with visable large pores formed internal. After immersed in PBS for 7 days (Fig. 1c), small crystals grew bigger and occupated the space of large pores, which turn the visable pores into micropores such as irregular wool stoma and gel pore [23]. Among the 3 cement groups, 1-HA/CPC showed the densest microstructure either before or after being immersed in PBS.

XRD patterns of the cements after immersion in PBS for 7, 14 and 21 days are shown in Fig. 2 A-C, and the pattern of commecial hydroxyapatite was used as a reference. The as-prepared cements showed no obvious sign of hydroxyapatite formation. After being immersed for 7 days, diffraction peaks corresponding to the main peaks in the reference hydroxyapatite emerged at ~25.90° and ~31.96° (2θ), indicating continuing of hydration reaction and conversion of the hydroxyapatite like material. At the same time, the intensity and height of the diffraction peaks were broad and weak as compared with those of the reference hydroxyapatite, which indicated the incomplete crystallization of primary hydroxyapatite or the size of hydroxyapatite microcrystals within the nanometer range, or both reasons [20]. After being immersed for 14 and 21 days, the main peaks at ~25.90° and ~31.96° (2θ) became higher and sharper for all the cement groups, and there was no measurable difference in the location of main peaks among CPC, 1-HA/CPC and 4-HA/CPC (Fig. 2A-C). For each time point, the diffraction peak of 1-HA/CPC and 4-HA/CPC sample was sharper and more

Table 3
Handling properties of hyaluronic acid/calcium phosphate cements (results were expressed as mean ± SD).

Cement Group	Ij (%)[a]	IST (min)[b]
CPC	65.63 ± 3.51	27.24 ± 0.98
1-HA/CPC	83.61 ± 4.36	23.63 ± 0.76
4-HA/CPC	85.13 ± 3.89	24.56 ± 0.69

[a] : Injectability (Ij).
[b] : Initial setting time (IST).

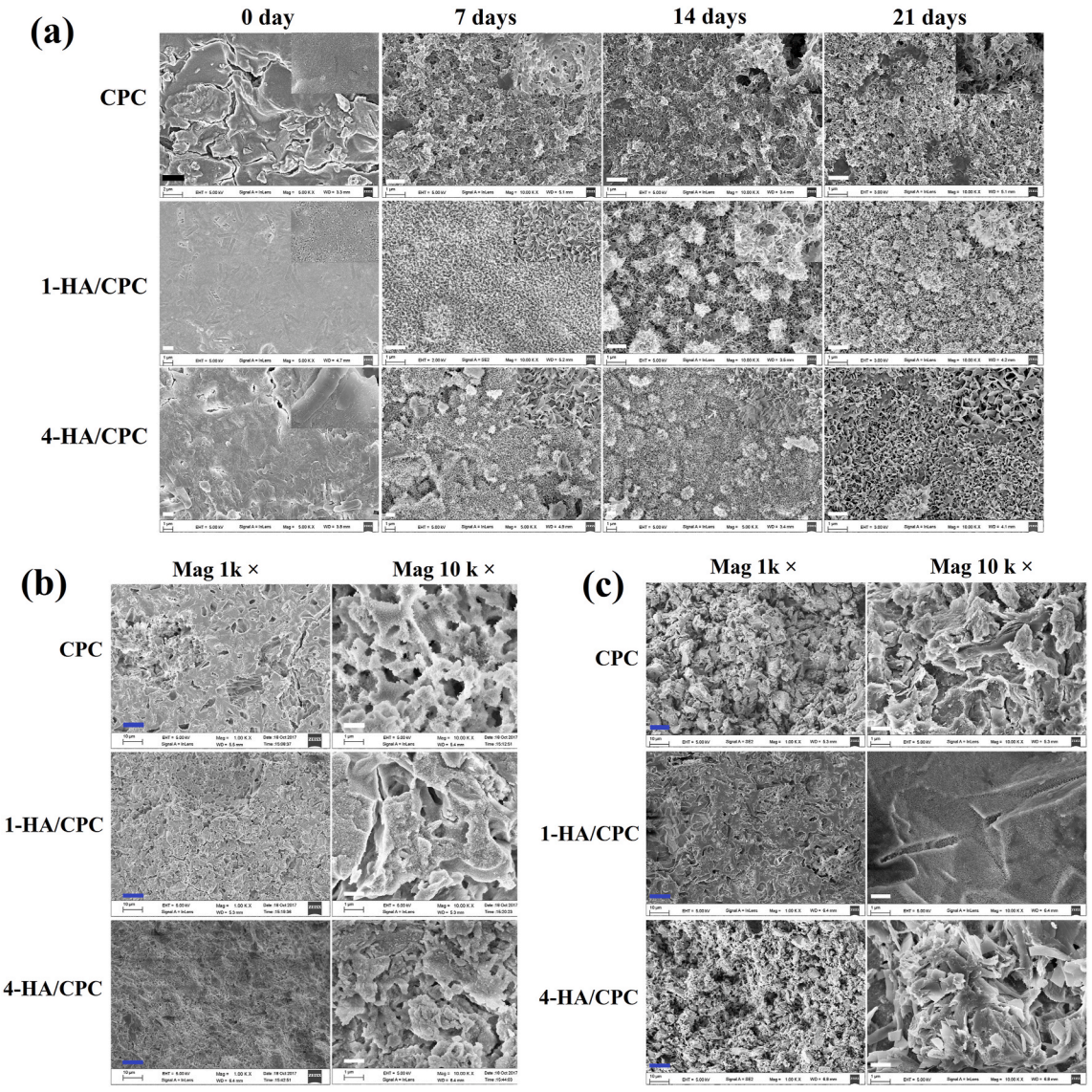

Fig. 1. Surface morphology of hyaluronic acid/calcium phosphate cements with different immersing time in PBS (a); and morphology of cross-sections of hyaluronic acid/calcium phosphate cements before (b) and after immersing in PBS for 7 days (c), black scale bar at 2 μm, white scale bar at 1 μm and blue scale bar at 10 μm.

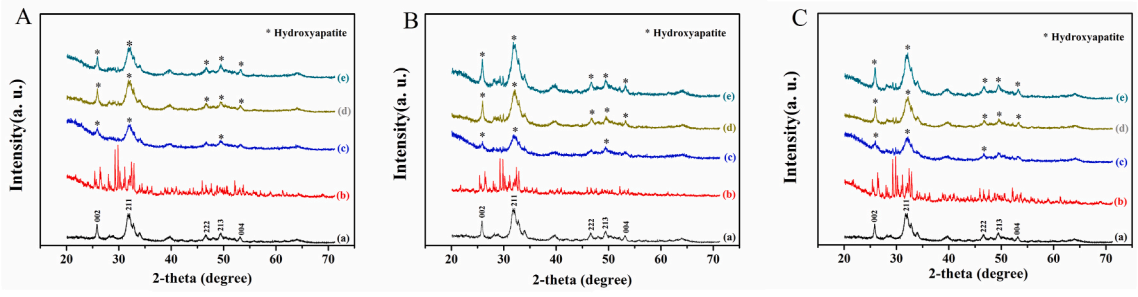

Fig. 2. X-ray diffraction patterns of (A) CPC, (B) 1-HA/CPC and (C) 4-HA/CPC cements before and after immersion in PBS for 0, 7, 14 and 21 days. (a)Hydroxyapatite; (b) as prepared cement before immersion; cements immersed in PBS for 7 days (c), 14 days (d) and 21 days (e).

intense than that of the CPC, which gave a solid proof about the accelerated hydration rate of hydroxyapatite by hyaluronic acid incorporation [15].

3.3. Compressive strength

Compressive strength of the cements, as prepared and after being immersed for up to 21 days in PBS is shown in Fig. 3. Compressive strength of all the cements increased rapidly in PBS during the initial periods of 14 days, and showed no significant uprating with prolonged

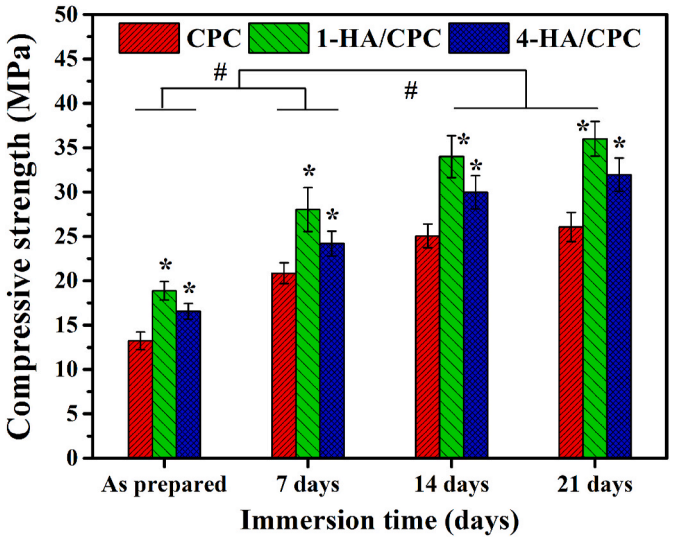

Fig. 3. Compressive strength of hyaluronic acid/calcium phosphate cements before and after immersion in PBS (Mean ± SD; n = 5; #significant difference among different immersion days in PBS, $p < 0.05$; * significant difference compared with CPC groups, $p < 0.05$).

immersion time. For both of the as prepared and immersed samples, 1-HA/CPC showed the highest compressive strength (18.87 ± 1.03 MPa and 36.00 ± 1.97 MPa respectively), and CPC showed the lowest compressive strength values (13.23 ± 0.99 MPa and 26.06 ± 1.64 MPa respectively).

3.4. Adhesion and proliferation of hBMSCs in vitro

After cultured for 1 and 24 h (Fig. 4a), hBMSCs revealed numerous lamellipodia and filopodia on surface of all cement groups, exhibiting suitable cytocompatibility of the cement groups. After being cultured with cement extracts for 1, 3 and 5 days, relative growth rates (RGRs) of all the cement extracts were higher than the acceptable value (dashed line in Fig. 4b, RGRs = 70%) according to ISO 10993, as normalized to the control group (cell medium without extract, RGR 100%). The RGRs were 89.10 ± 1.79, 84.21 ± 1.53, 79.75 ± 4.49 for CPC, 1-HA/CPC and 4-HA/CPC respectively for cultured time of 1 day. With the prolonged cultured time, the RGRs were 95.09 ± 4.71, 90.54 ± 2.12, 86.99 ± 1.31 for CPC, 1-HA/CPC and 4-HA/CPC respectively for cultured time of 5 days. Even though extracts of CPC group had higher RGRs than that of 1-HA/CPC and 4-HA/CPC groups for all the culuture time, there was no significant differences for RGRs among the three cements.

3.5. ALP staining and ALP activities of hBMSCs in vitro

ALP expression of hBMSCs after being co-cultured for 7 days on the sample surface was positive for all the cements and the control group (Fig. 5). The control group (cell medium without extract) revealed the biggest stained area of ALP when compared with cement groups. The stained area of ALP for 1-HA/CPC and 4-HA/CPC groups were also more than that of CPC group at the culturing time of 7 days. Besides, 4-HA/CPC showed the highest staining area among the cement groups (Fig. 5a). ALP activity exhibited similar tendency to ALP staining results (Fig. 5b).

3.6. Osteogenesis-related protein and genes expression of hBMSCs in vitro

The OPN and RUNX-2 expression of hBMSCs after being co-cultured with cement samples for 7 days in OIM is presented in Fig. 6a and b. As showed by IF staining results, 1-HA/CPC and 4-HA/CPC groups had much higher RUNX-2 and OPN secretion than CPC group, and 4-HA/CPC group revealed the most RUNX-2 and OPN protein expression, which was consistent with ALP expression results. The osteogenesis-related genes expression (RUNX-2, ALP and OPN) of hBMSCs after being co-cultured with cements is showed in Fig. 6c–e. In general, incorporating HA into CPC promoted the expression of osteogenesis-related genes of hBMSCs for all the culture time points. However, at the culture time of 7 days, 1-HA/CPC group showed the highest RUNX-2 expression of hBMSCs, and 4-HA/CPC group revealed the lowest RUNX-2 expression of hBMSCs (Fig. 6c). After being cultured for 14 and 21 days, expression of RUNX-2, ALP and OPN for 1-HA/CPC and 4-HA/CPC groups was both much higher than CPC group (Fig. 6c–e). At the meanwhile, 4-HA/CPC group revealed the most effective stimulation on ALP and OPN expression of hBMSCs.

3.7. Microcomputed tomography (micro-CT) of cements after implantation in vivo

micro-CT images and 3D computer models of tibial defects after implantation for 4, 8 and 12 weeks were investigated to evaluate bone regeneration, and the results were showed in Fig. 7. New bone formation (yellow area) was shown around the surface of cylindrical specimens at each implantation time. Four weeks after implantation, a small amount of regenerated osseous tissue was observed, and there was no distinct difference for new bone formation among the three cement groups. Large amount of new bone formation around the implants was detected at 8 and 12 weeks after implantation. In comparison, there was more extensive new bone formation around the implants for 1-HA/CPC and 4-HA/CPC groups compared to CPC group. Moreover 4-HA/CPC group showed the highest amount of new bone formation for both of 8 and 12 weeks after implantation. Quantitation of the micro-CT images (Table 4) exhibited that, CPC group showed the lowest BV/TV (2.53 ± 0.12), Tb. pf (0.017 ± 0.001) and BMD (190.31 ± 12.71) values, and 4-HA/CPC group showed the highest BV/TV (5.31 ± 0.08), Tb. pf (0.020 ± 0.001) and BMD (248.74 ± 39.47) values at the implantation time of 4 weeks. Increasing values of BV/TV, Tb. pf and BMD values were depicted with the prolonged implantation time. At implantation time of 12 weeks, the values of BV/TV, Tb. pf and BMD for CPC group was 4.53 ± 0.12, 0.022 ± 0.001 and 238.03 ± 43.55 respectively, and the values of BV/TV, Tb. pf and BMD for 4/HA-CPC group was 11.26 ± 0.05, 0.035 ± 0.002 and 264.06 ± 45.13 respectively. For all the selected timepoint, 4-HA/CPC group demonstrated the highest bone microarchitecture values except the Tb. pf of 1-HA/CPC with implantation time of 8 weeks.

3.8. Histological analysis of bone repair ability in vivo

The bone-cement interface in the rat tibia defects 4, 8 and 12 weeks after implantation of CPC, 1-HA/CPC and 4-HA/CPC cements was further assessed with histomorphometric analysis. As showed in Hematoxylin-eosin (H&E) (Fig. 8 a-c) and Masson's trichrome (MT) (Fig. 8 d-f) stained sections, none of the cements showed sign of rejection, necrosis or infection after implantation, which indicated their satisfying biocompatibility at the defect sites. At implantation time of 4 weeks (Fig. 8 a and d), CPC group showed rare new bone formation, while 1-HA/CPC and 4-HA/CPC groups exhibited relatively more new bone formation with dense mineralization (areas stained red in MT staining) *in vivo*. Moreover, new bone permeated into the implants of 4-HA/CPC group and blood vessels also emerged in the new formed bone (as indicated by blue arrows in H&E and magenta arrows in MT staining). More new bone formed around the peripheral area of implants for all the cement groups with longer implantation time. For CPC group, there was abundant fibrous tissue existing around the boundaries between the implant and host bone (Fig. 8 b and e) after 8 weeks. After implantation of 8 and 12 weeks (Fig. 8 b and c, Fig. 8 e and f), 1-HA/CPC and 4-HA/CPC groups showed large amount of dense calcified new bone (area stained red) and bold vessel formation (as indicated by arrows). Histological studies revealed that cements incorporating HA integrated

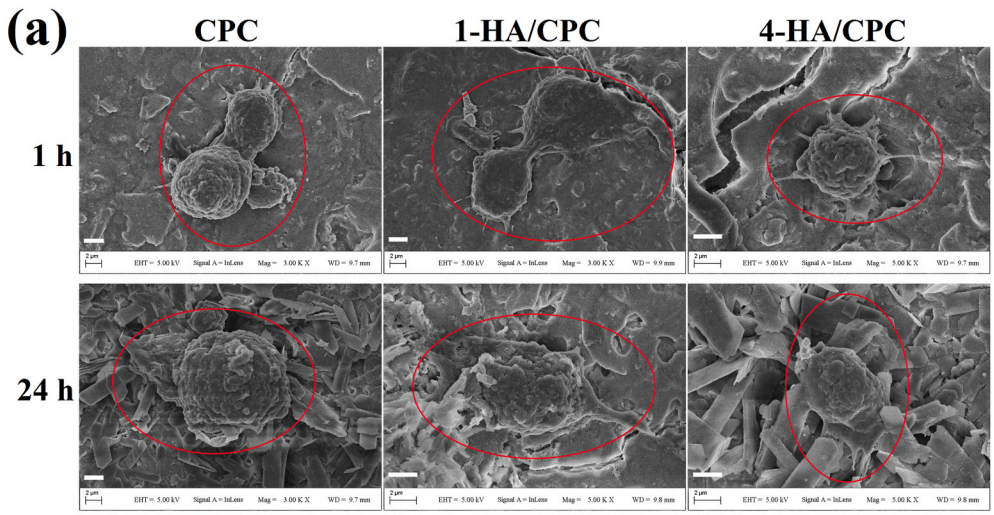

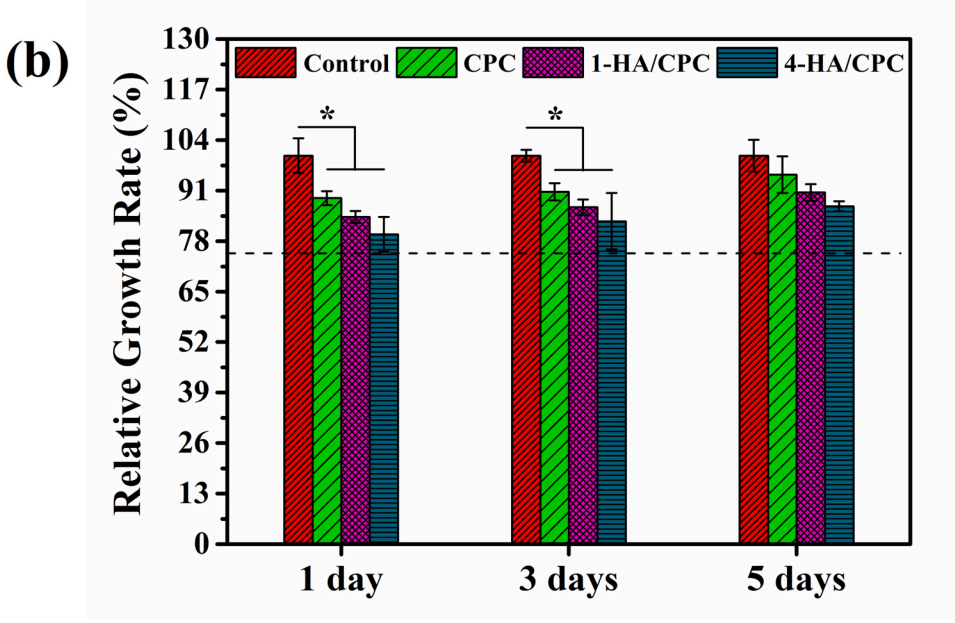

Fig. 4. SEM images showing adhesion of hBMSCs on the surface of hyaluronic acid/calcium phosphate cements after being cultured for 1 h and 24 h, scale bar at 2 μm (a); and relative growth rate (RGR) of hBMSCs after being cultured in extract solutions of hyaluronic acid/calcium phosphate cements for 1, 3 and 5 days; cell medium without extract was used as the control (the dashed line indicates acceptable RGR with value of 70% according to ISO 10993). (results were expressed as Mean ± SD; n = 5; *significant difference compared with CPC group, $p < 0.05$).

well with the host bone after implantation, and resulted in improved bone regeneration than pure CPC in the defect zone.

3.9. Immunohistochemical analysis of cement implants in vivo

Fig. 9 exhibits the immunohistochemical analysis of rat tibia defects implanted with CPC, 1-HA/CPC and 4-HA/CPC for 4, 8 and 12 weeks. Immunohistochemical staining revealed positive expression of Col-1, OCN and BMP-2 for all the cement groups, and those osteogenic-related protein expression mainly occurred in direct vicinity of the implants towards the biomaterial-metaphyseal cancellous (distal) bone and mid cortical regions, especially with longer implantation time. HA incorporation significantly enhanced expression of Col-1, OCN and BMP-2 in 1-HA/CPC and 4-HA/CPC groups compared to CPC group. At the implantation time of 4, 8 and 12 weeks (Figure 9a), 1-HA/CPC and 4-HA/CPC groups exhibited stronger positive expression of Col-1, OCN and BMP-2, as evidenced in Fig. 9 b and **c**. Quantitation of immunohistochemical analysis results (Fig. 9d–f) showed that COL-1, OCN and BMP-2 expression in the defects implanted with 1-HA/CPC and 4-HA/CPC groups was significantly stronger than that for CPC group, and 4-HA/CPC group showed the highest amount of Col-1, OCN and BMP-2 expression.

4. Discussion

Hyaluronic acid, as a natural linear glycosaminoglycan and well received biomedical materials, was introduced into CPC in a few researches to improve its physicochemical properties and/or biological performance [4–8]. Zhang and coworkers found that, injectable paste formula with appropriate comprehensive property can be achieved by moderating crosslinked sodium hyaluronate (cHA) solution and hydroxyapatite (HAp) spherical particles [24]. Yang and coworkers developed a cell carrier hydrogel composed of porous tricalcium phosphate (TCP) particle and hyaluronic acid (HA) gel. After loaded with fat cells, this composite hydrogel can maintain activity of fat cells and further support its proliferation, which showed a prospective application in tissue engineering [25].

While these results are inspiring, the *in vivo* studies still need to and biological mechanism of enhancement on bone formation of hyaluronic acid incoporating into calcium phosphate cement is rare to be determined. So in this study, hyaluronic acid (HA) was added in the initial setting liquid to evaluate its enhancement in physicochemical properties and discuss the underlying biological mechanism of stimulation on osteogenic capacity of CPC. In details, the added HA significantly accelerated the remodeling and formation of HA in CPC matrix. The

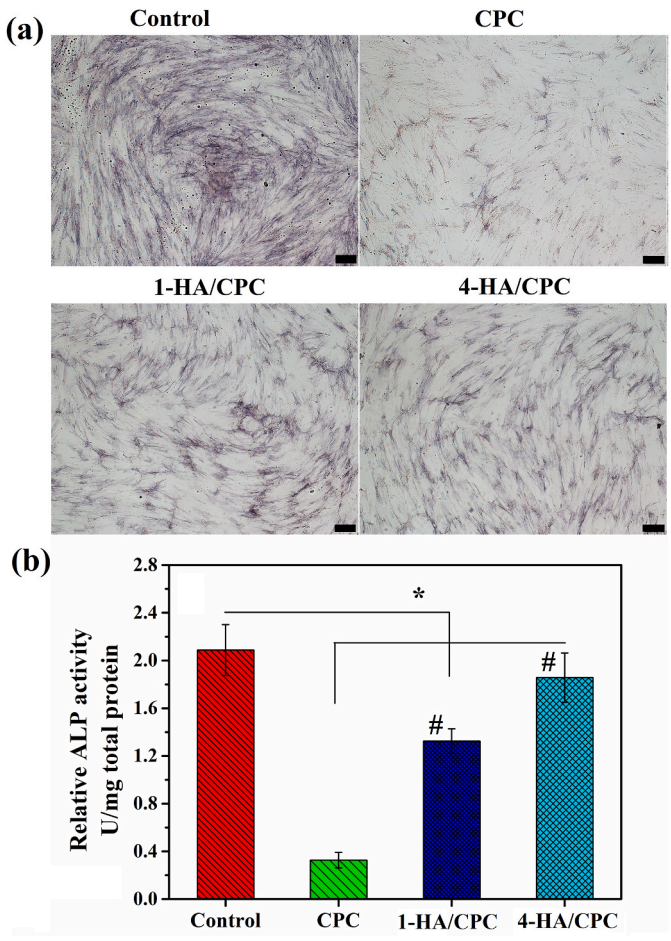

Fig. 5. ALP staining (a) and quantitative assay of ALP activity (b) of hBMSCs co-cultured with hyaluronic acid/calcium phosphate cements in OIM for 7 days, cell medium without extract was used as the control and scale bar at 200 μm. (results were expressed as Mean ± SD; n = 5; *significant difference between control and cement groups, $p < 0.05$; #significant difference among cement groups, $p < 0.05$).

formation of bone-like apatite is believed to be an essential criteria for bone substitues, since bone is mainly made up of apatite-like minerals, biomemics of its natural inorganic components is therefore generally understood in the construction of bone [22]. As expected, after immersed in PBS, apatite-like minerals were detected on cements surface which was faciliated with the incorporation of HA (Fig. 1), higher amount and maturer morphology of the crystalline-apatite was observed with time (Fig. 2). Here, the added HA seemed to serve as a solvent to accelerate the growth of hydroxyapatite by acclerating the dissolving of initial calcium phosphates, as observed by bigger particle size (Fig. 1) and indicated by sharper diffraction peaks (Fig. 2) both in 1-HA/CPC and 4-HA/CPC groups, which was consistent with the previous report, that was, HA could promot the ion exchange to speed up crystal growth of hydroxyapatite because of enhanced supersaturation degree of Ca^{2+} and PO_4^{3-} ions [15,26]. As a result, the formation of apatite-like minerals might further stablize its native poor mechanical strength of CPC itself.

Up to now, the clinical criteria for mechanical standard of bone substitutes is still puzzled, since the load in bone varies with the location and its own biological function. The ideal bone substitutes can play the key factor to initially reinforce the bone defects, with time, further induce bone ingrowth and eventually to be replaced by the newly formed bone. As such, the difficulty lies in the dilemma to measure the required mechanical quality of the bone to initial fixation, but the essential fixation ability and further increased ability for bone ingrowth are particularly in need [27]. As a result, the maximal enhancement of its mechanical property is anticipated to firstly stabilize the essential reinforcement of the bone defects, at least to avoid the crack or collapse the bone defects.

The added HA significnatly enhanced the compressive strength of CPC. As expected, after immersed in PBS, the compressive strength of all cements increased substantially with time (Fig. 3), that is definetly associated with the increased conversion rate of hydroxyapatite [23]. Here 1-HA/CPC group showed obvously better compressive strength (29.04 ± 4.48 MPa and 36.00 ± 5.37 MPa respectively) than that of CPC group (17.2 ± 0.39 MPa and 25.98 ± 1.77 MPa respectively) both before and after immersion. It indicates the enhancement of its anti-washout property of the cements was well modified, since the compressive strength of the cements increased significantely. Such result may attribute to the higher anchoring strength inside the cement matrix accompanied with improved cohesiveness with HA incorporation [24]. However the overloaded HA was found to compromise the integration of the cement matrix, which was possibly with lower supersaturation degree of calcium and phosphate by the overloaded HA, thus retarding the formation of apatite, although showing better mechanical strength than unloaded-HA cements of the CPC, but still substantially lower than that of the property with lower loaded.

More important, the cements added with HA showed better genes expression of hBMSCs *in vitro* as well as its ALP activity and OPN expression, thus stimulated more new bone formation in the tibia of rats. More hBMSCs expressed better attaching and spreading ability on the surface of 1-HA/CPC and 4-HA/CPC groups (Fig. 4).

However, there was also detected the slightly declined cell activity for both 1-HA/CPC and 4-HA/CPC groups as compared with CPC group (Fig. 4b), which indicated that HA sometimes might not be happy to promote the proliferation of bone related cells, as reported previously by Zhao and Xu [17,28]. On the other hand, the incorporation of HA in all contents obviously enhanced ALP activity (Fig. 5) and osteogenic differentiation related protein expression (Fig. 6a) of hBMSCs, and the optimal enhancement was observed in 4-HA/CPC group. The related marker of ALP, OPN and RUNX-2 well expressed the activation of related genes and suggested that the incorporation of HA could enhance bone ECM (extracellular matrix) synthesis and osteogenic differentiation of hBMSCs [17].

After implantion, hydroxyapatite conversion of CPC will facilitate proteins deposition and further offeres a biointerface to support recruitment of bone related cell and deposition of bone matrix [23]. HA incorporating showed a higher osteogenic capacity for cement groups of 1-HA/CPC and 4-HA/CPC, as indicated by more new bone and vascular formation around the implants *in vivo* (Fig. 8). Consistent with results of cell culture assays *in vitro*, 4-HA/CPC cement group also showed the highest efficiency in stimulating osteogenesis and angiogenesis in the bone defects, and enhancement in osteogenesis may effectively improve the fixation of implant, reduce bone resorption and promote the formation of stable interface [29,30]. Details from immunohistochemical staining (Fig. 9a) and semi-quantitative assays (Fig. 9b) showed that better osteogenesis of 1-HA/CPC and 4-HA/CPC may result by higher osteogenic protein (COL-1, OCN and BMP-2) expression with added HA.

As one of the main components of ECM in connective tissues, HA was reported to interact with receptors such as CD44 to stimulate differentiation [31,32], migration and vascularization of endothelial cells [33], which in turn favors bone regeneration. Moreover, HA can play a key role to maintain growth factors such as TGF-β within the local environment to affect tissue regeneration positively [18]. On the basis, it is reasonable to presume that the underlying biological mechanism of hyaluronic acid affected bone repair ability of calcium phosphate cement may as followed: HA added in cement implants may capture MSCs and endothelial cells, and further stimulate osteogenic factors secrection and osteogenic genes expression to accelerate new bone formation.

The results have shown that in the tibia, addition of HA in the CPC material may provide a more favorable microenvironment for cell

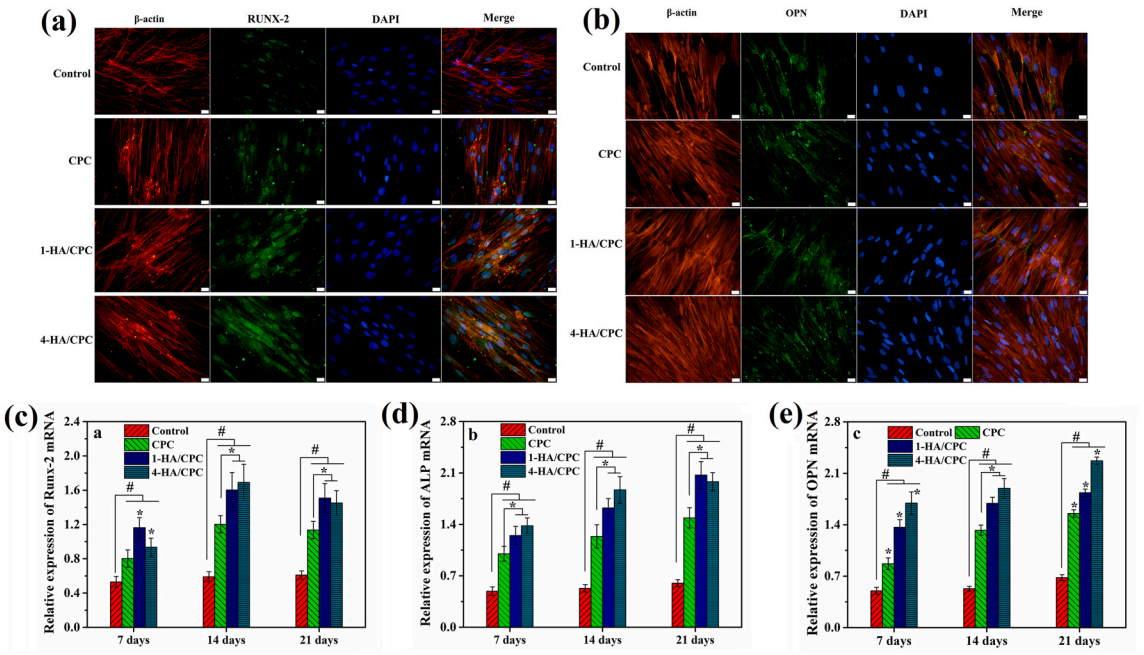

Fig. 6. Immunofluorescence assay (IF) staining of RUNX-2 (a) and OPN (b) protein expression of hBMSCs after being cultured with hyaluronic acid/calcium phosphate cements in OIM for 7 days, cell medium without extract was used as the control and scale bar at 20 μm; and the osteogenic-related gene expression of hBMSCs after being co-cultured with hyaluronic acid/calcium phosphate cements in OIM, (c): Runx-2; (d): ALP; (e): OPN. (results were expressed as Mean ± SD; n = 5; *significant difference among cements group, $p < 0.05$; # significant difference compared with Control group, $p < 0.05$).

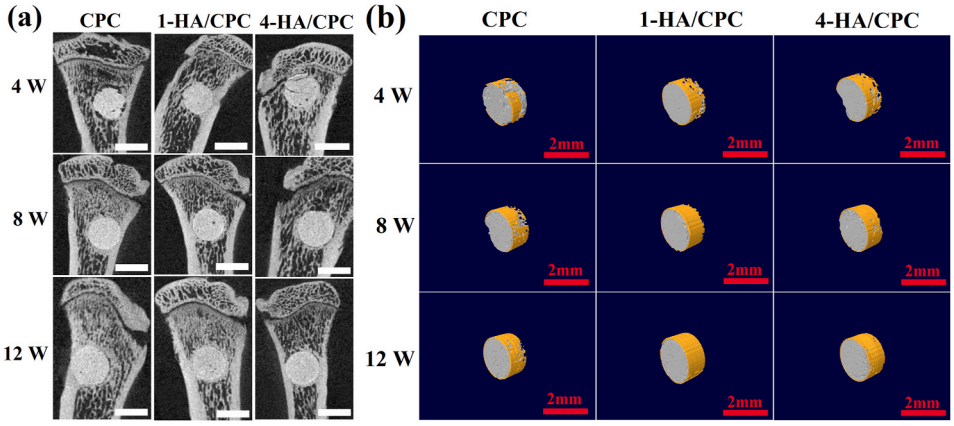

Fig. 7. Sagittal images (a) and 3D reconstructed images (b) by micro-CT imaging of the area surrounding cement implants, showing newly formed bone at different distances from edge of the cement 4, 8 and 12 weeks after implantation for in rat tibial defects, white and red scale bar both at 2 mm. (Yellow area presenting new bone formation in (b)). (For interpretation of the references to colour in this figure legend, the reader is referred to the Web version of this article.)

Table 4
Bone structural parameters of the rat tibia defects with cement implantation (statistical results, and results were expressed as mean ± SD).

Bone structure parameters		4 W	8 W	12 W
BV/TV[a]	CPC	2.53 ± 0.12	3.82 ± 0.07	4.53 ± 0.12
	1-HA/CPC	3.42 ± 0.15	4.53 ± 0.05	5.96 ± 0.21
	4- HA/CPC	5.31 ± 0.08	6.39 ± 0.07	11.26 ± 0.05
Tb.pf[b]	CPC	0.017 ± 0.001	0.020 ± 0.001	0.022 ± 0.001
	1- HA/CPC	0.020 ± 0.001	0.022 ± 0.002	0.028 ± 0.002
	4- HA/CPC	0.020 ± 0.002	0.024 ± 0.002	0.035 ± 0.002
BMD[c]	CPC	190.31 ± 12.71	214.25 ± 23.43	238.03 ± 43.55
	1- HA/CPC	216.26 ± 28.95	238.21 ± 63.25	238.13 ± 33.38
	4- HA/CPC	248.74 ± 39.47	233.38 ± 51.04	264.06 ± 45.13

[a] : Bone volume/total volume (BV/TV, %).
[b] : Bone trabecular pattern factor (Tb.pf, mm^{-1}).
[c] : Bone mineral density (BMD, mg/cm^3).

attachment and differentiation, and improve the osteogenic capability. However, the phase composition of bone cement was not characterized *in vivo* as a function of implantation time, and so, the phase transition of hydroxyapatite after implantation could not be tracked. Also the biomechanical tests were not performed on the excised specimens for determining the stability of the bone-implant interface. Future study will focus on these issues with more further research.

5. Conclusion

Hyaluronic acid (HA) incorporated into bone cements composed of biphasic phosphate and a citric acid setting liquid was exhibited to offer an approach to affect physicochemical properties and osteogenesis of the cements. An increase in HA incorporation (from 0 to 1 (w/v) % HA in the citric acid setting liquid) resulted in higher compressive strength and better cohesiveness of the cements. When immersing in PBS, the

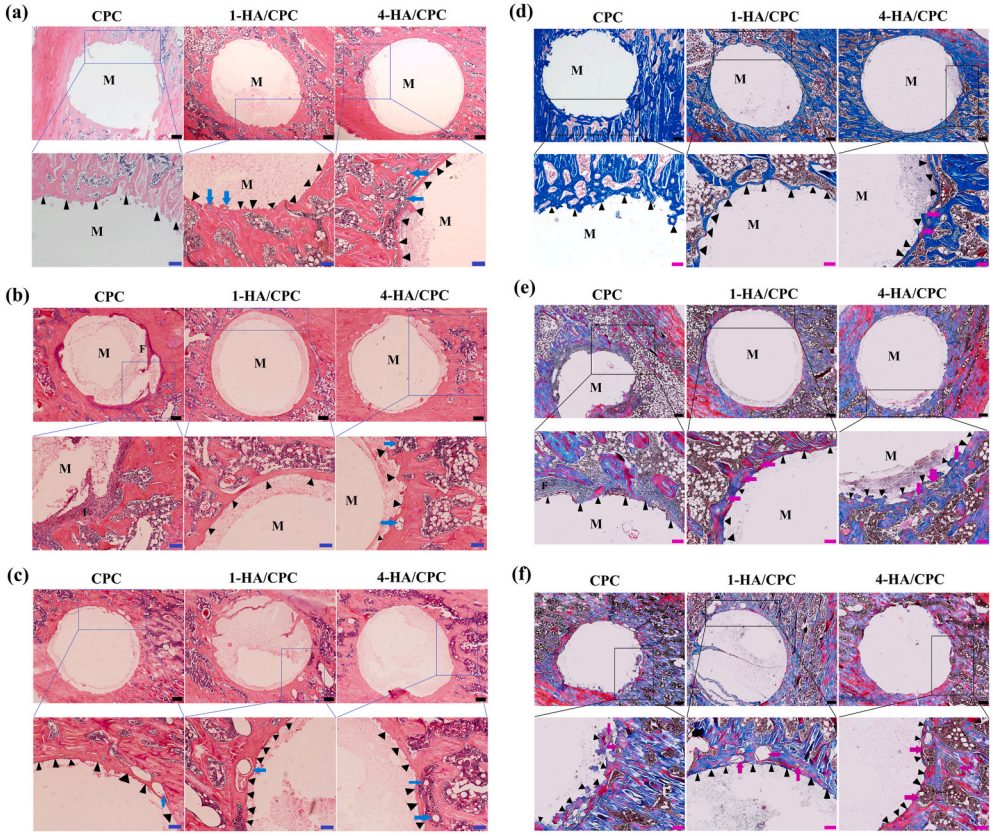

Fig. 8. Hematoxylin-eosin staining (H&E staining) of the bone tissue with implanted cements for 4 (a), 8 (b) and 12 weeks (b); and Masson's trichrome staining (MST) of the bone tissue with implanted cements for 4 (c), 8 (d) and 12 weeks (e), dense calcified new bone was stained red, while collagen-rich tissues were stained blue, black scale bar at 200 μm, blue and magenta scale bar at 100 μm. (F: fibrous tissue; M: cement specimens; Triangles indicate new bone formation around the boundaries between implant and host bone; Magenta arrows indicate vascular formation). (For interpretation of the references to colour in this figure legend, the reader is referred to the Web version of this article.)

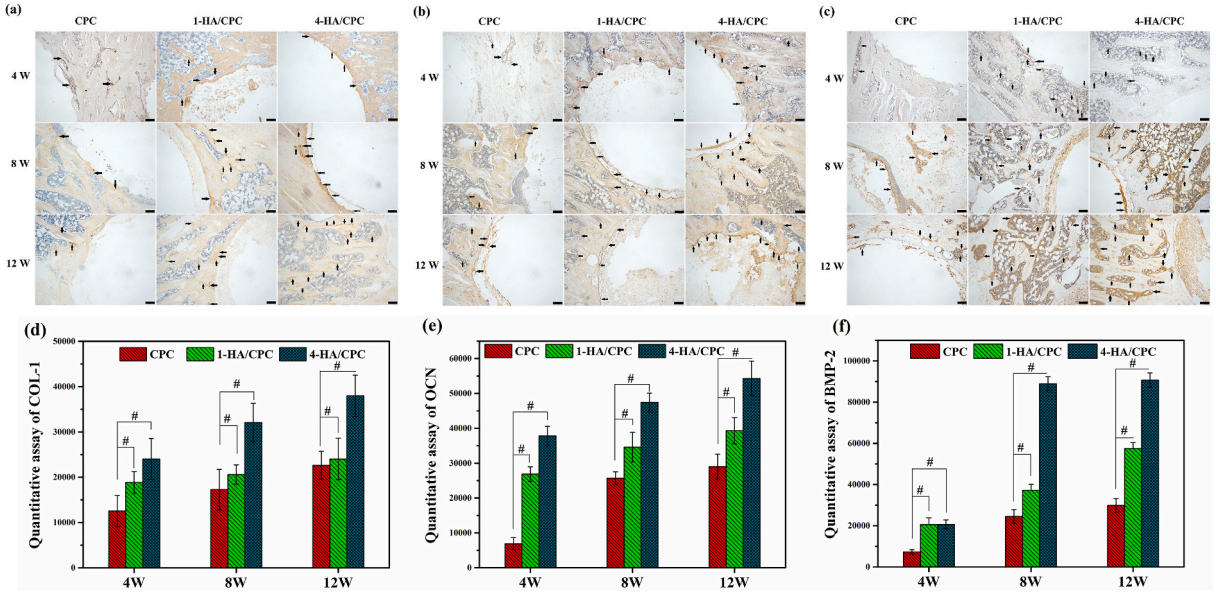

Fig. 9. Immunohistochemical staining for COL-1 (a), OCN (b) and BMP-2 (c) with implanted cements for 4, 8 and 12 weeks. Black arrows indicate positive expression of these proteins (yellow area in images, scale bar at 100 μm). Quantitative assay of protein expression for COL-1 (d), OCN (e) and BMP-2 (f). (Mean ± SD; n = 5; # significant difference compared with CPC group, $p < 0.05$). (For interpretation of the references to colour in this figure legend, the reader is referred to the Web version of this article.)

conversion rate to hydroxyapatite significantly increased, as well as the content of hydroxyapatite. HA incorporating into the cements stimulated ALP activity, osteogenic related protein and mRNA expression of hBMSCs *in vitro*. Material components with the best osteogenic activity were achieved in the cement with 4 w/v % HA incorporated in the citric acid setting liquid (designated as 4-HA/CPC). After being implanted in rat tibial defects, 4-HA/CPC cements exhibited more bone formation compared to CPC and 1-HA/CPC cement groups. The underlying biological mechanism of this stimulation for HA/CPC may be on account of higher osteogenic promoting factors secretion and osteogenic genes expression with hyaluronic acid incorporation. These results proved that hyaluronic acid is an effective bone cement additive material to acquire

better physicochemical and biological properties than traditional calcium phosphate cement.

CRediT authorship contribution statement

Xu Cui: and. **Chengcheng Huang:** and. **Zhizhen Chen:** contributed to the experimental planning, performed the experiments, analyzed the data, and wrote the main manuscript text. Haobo Pan supervised the project, contributed to the experimental planning, provided funding and intellectual input and edited the main manuscript text. **Meng Zhang:** All authors read and approved the final manuscript. **Chunyu Liu:** contributed to the experimental planning and analyzed the data. . **Kun Su:** contributed to the experimental planning and analyzed the data. . **Jianyun Wang:** contributed to the experimental planning and analyzed the data. . **Li Li:** contributed to the experimental planning and analyzed the data. . **Renxian Wang:** contributed to the experimental planning and analyzed the data. . **Bing Li:** and. **Dafu Chen:** and. **Changshun Ruan:** and. **Deping Wang:** and. **William W. Lu:** contributed to the intellectual input, scientific discussion. Meng Zhang. **Haobo Pan:** All authors read and approved the final manuscript.

Declaration of competing interest

The authors declared that they have no conflicts of interest to this work.

Acknowledgements

This study was supported by the National Key R&D Program of China (Grant No. 2018YFC1106300 and 2017YFC1105000), the National Natural Science Foundation of China (Grant No. 52072398, 51802340, 31870956, 81860385, 81672227, U2001221, 51772210), the Frontier Science Key Research Programs of CAS (Grant No. QYZDB-SSW-JSC030), the Shenzhen Significant Strategy Layout Project (Grant No. JCYJ20170413162104773 and JCYJ20200109114620793), Beijing Municipal Health Commission (Grant No. BMHC-2018-4, BMHC-2019-9, PXM2020_026275_000002).

References

[1] M. Zhang, J.P. Matinlinn, J.K.H. Tsoi, W.L. Liu, X. Cui, W.W. Lu, H.B. Pan, Recent developments in biomaterials for long-bone segmental defect reconstruction: a narrative overview, J. Orthop. Translat. 20 (2020) 26–33.
[2] Y.k. Yu, Y. Wang, W.D. Zhang, H. Wang, J.Y. Li, L.B. Pan, F.X. Han, B. Li, Biomimetic periosteum-bone substitute composed of preosteoblast-derived matrix and hydrogel for large segmental bone defect repair, Acta Biomater. 113 (1) (2020) 317–327.
[3] H.H.K. Xu, P. Wang, L. Wang, C.Y. Bao, Q.M. Chen, M.D. Weir, L.C. Chow, L. Zhao, X.D. Zhou, M.A. Reynolds, Calcium phosphate cements for bone engineering and their biological properties, Bone Res 5 (2017) 17056.
[4] H.J. Lee, B. Kim, A.R. Padalhin, B.T. Lee, Incorporation of chitosan-alginate complex into injectable calcium phosphate cement system as a bone graft material, Mater. Sci. Eng. C 94 (2019) 385–392.
[5] Y.J. No, X.Z. Xin, Y. Ramaswamy, Y.H. Li, S. Roohaniesfahani, S. Mustaffa, J. Shi, X.Q. Jiang, H. Zreiqat, Novel injectable strontium-hardystonite phosphate cement for cancellous bone filling applications, Mater. Sci. Eng. C 97 (2019) 103–115.
[6] L. Li, X.Z. Peng, Y.B. Qin, R.C. Wang, J.L. Tang, Xu Cui, T. Wang, W.L. Liu, H. B. Pan, B. Li, Acceleration of bone regeneration by activating Wnt/β-catenin signalling pathway via lithium released from lithium chloride/calcium phosphate cement in osteoporosis, Sci. Rep. 7 (2017) 45204.
[7] K. Xiong, J. Zhang, Y.Y. Zhu, L. Chen, J.D. Ye, Zinc doping induced differences in the surface composition, surface morphology and osteogenesis performance of the calcium phosphate cement hydration products, Mater. Sci. Eng. C 105 (2019) 110065.
[8] S. Wang, C. Xu, S.C. Yu, X.P. Wu, Z. Jie, H.L. Dai, Citric acid enhances the physical properties, cytocompatibility and osteogenesis of magnesium calcium phosphate cement, J Mech Behav Biomed Mater 94 (2019) 42–50.
[9] D. Arcos, A.R. Boccaccini, M. Bohner, A. Díez-Pérez, M. Epple, E. Gómez-Barrena, A. Herrera, J.A. Planell, L. Rodríguez-Mañas, M. Vallet-Regí, The relevance of biomaterials to the prevention and treatment of osteoporosis, Acta Biomater. 10 (5) (2014) 1793–1805.
[10] X.P. Wang, L. Chen, H. Xiang, J.D. Ye, Influence of anti-washout agents on the rheological properties and injectability of a calcium phosphate cement, J. Biomed. Mater. Res. B Appl. Biomater. 81B (2007) 410–418.
[11] T.Y. Chiang, C.C. Ho, D.C. Chen, M.H. Lai, S.J. Ding, Physicochemical properties and biocompatibility of chitosan oligosaccharide/gelatin/calcium phosphate hybrid cements, Mater. Chem. Phys. 120 (2–3) (2010) 282–288.
[12] G.W. Qian, X.M. Li, F.P. He, J.D. Ye, Improving the anti-washout property of calcium phosphate cement by introducing konjac glucomannan/kappa-carrageenan blend, J. Biomater. Appl. 33 (2019) 1094–1104.
[13] M.H. Alkhraisat, C. Rueda, F.T. Mario, J. Torres, E.L. Cabarcos, The effect of hyaluronic acid on brushite cement cohesion, Acta Biomater. 5 (2009) 3150–3156.
[14] D. Petta, G. Fussell, L. Hughes, D.D. Buechter, C.M. Sprecher, M. Alini, D. Eglin, M. D'Este, Calcium phosphate/thermoresponsive hyaluronan hydrogel composite delivering hydrophilic and hydrophobic drugs, J. Orthop. Translat. 5 (2016) 57–68.
[15] K. Suzuki, T. Anada, T. Miyazaki, N. Miyatake, Y. Honda, K.N. Kishimoto, M. Hosaka, H. Imaizumi, Eiji Itoi, O. Suzuki, Effect of addition of hyaluronic acids on the osteoconductivity and biodegradability of synthetic octacalcium phosphate, Acta Biomater. 10 (2014) 531–543.
[16] M. Liu, X. Zeng, C. Ma, H. Yi, Z. Ali, X.B. Mou, S. Li, Y. Deng, N.Y. He, Injectable hydrogels for cartilage and bone tissue engineering, Bone Res 5 (2017) 17104.
[17] N.B. Zhao, X. Wang, L. Qin, Z.Z. Guo, D.H. Li, Effect of molecular weight and concentration of hyaluronan on cell proliferation and osteogenic differentiation in vitro, Biochem. Biophys. Res. Commun. 465 (2015) 569–574.
[18] T. Sasaki, C. Watanabe, Stimulation of osteoinduction in bone wound-healing by high-molecular hyaluronic-acid, Bone 16 (1995) 9–15.
[19] D.C. West, I.N. Hampson, F. Arnold, S. Kumar, Angiogenesis induced by degradation products of hyaluronic-acid, Science 228 (1985) 1324–1326.
[20] X. Cui, Y.D. Zhang, J.Y. Wang, C.C. Huang, Y.D. Wang, H.S. Yang, W.L. Liu, T. Wang, D.P. Wang, G.C. Wang, C.S. Ruan, D.F. Chen, W.W. Lu, W.H. Huang, M. N. Rahaman, H.B. Pan, Strontium modulates osteogenic activity of bone cement composed of bioactive borosilicate glass particles by activating Wnt/β-catenin signaling pathway, Bioact. Mater. 5 (2020) 334–347.
[21] T. Kokubo, H. Takadama, How useful is SBF in predicting in vivo bone bioactivity? Biomaterials 27 (15) (2006) 2907–2915.
[22] P. Wang, L. Zhao, J. Liu, M.D. Weir, X.D. Zhou, H.H.K. Xu, Bone tissue engineering via nanostructured calcium phosphate biomaterials and stem cells, Bone Res 2 (2014) 14017.
[23] Y.J. Wang, Biomedical Creamic Materials. South China University of Technology Press, 2010.
[24] Y. Liu, Y.H. Wu, H. Lin, Y.M. Xiao, X.D. Zhu, K. Zhang, Y.J. Fan, X.D. Zhang, Study on an injectable biomedical paste using cross-linked sodium hyaluronate as a carrier of hydroxyapatite particles, Carbohydr. Polym. 195 (2018) 378–386.
[25] Y.C. Yang, C.C. Chen, W.C. Wu, W.L. Hsu, S.C. Tseng, Development of macroporous tricalcium phosphate with hyaluronic acid as the cell carrier as the subcutaneous filler, Ceram. Int. 43 (S1) (2017) S823–S828.
[26] Q. He, H.L. Chen, L. Huang, J.J. Dong, D.G. Guo, M.M. Mao, L. Kong, Y. Li, Z. X. Wu, W. Lei, N. Nuno, Porous surface modified bioactive bone cement for enhanced bone bonding, PloS One 7 (8) (2012) 1–11.
[27] X. Cui, C.C. Huang, M. Zhang, C.S. Ruan, S.L. Peng, L. Li, W.L. Liu, T. Wang, B. Li, W.H. Huang, M.N. Rahaman, W.W. Lu, H.B. Pan, Enhanced osteointegration of poly (methylmethacrylate) bone cements by incorporating strontium-containing borate bioactive glass, J. R. Soc. Interface 14 (131) (2017) 20161057.
[28] L. Huang, Y.Y. Cheng, P.L. Koo, K.M. Lee, L. Qin, J.C.Y. Cheng, S.M. Kumta, The effect of hyaluronan on osteoblast proliferation and differentiation in rat calvarial-derived cell cultures, J. Biomed. Mater. Res. 66A (15) (2015) 880–884.
[29] C. Capuccini, P. Torricelli, F. Sima, E. Boanini, C. Ristoscu, B. Bracci, G. Socol, M. Fini, I.N. Mihailescu, A. Bigi, Strontium-substituted hydroxyapatite coatings synthesized by pulsed-laser deposition: in vitro osteoblast and osteoclast response, Acta Biomater. 4 (6) (2008) 1885–1893.
[30] L. Maïmoun, T.C. Brennan, I. Badoud, D. Victor, R. Rizzoli, P. Ammann, Strontium ranelate improves implant osseointegration, Bone 46 (5) (2010) 1436–1441.
[31] P.B. Toole, Hyaluronan: from extracellular glue to pericellular cue, Nat. Rev. Canc. 4 (2004) 528–539.
[32] W.P. Noble, Hyaluronan and its catabolic products in tissue injury and repair, Matrix Biol. 21 (2002) 25–29.
[33] L.E. Pardue, S. Ibrahim, A. Ramamurthi, Role of hyaluronan in angiogenesis and its utility to angiogenic tissue engineering, Organogenesis 4 (4) (2008) 203–214.